DOI: 10.1002/cbic.200700045

Probing the Role of the DXDD Motif in Class II Diterpene Cyclases

Sladjana Prisic,[a] Jianjun Xu,[b, c] Robert M. Coates,[b] and Reuben J. Peters*[a]

Terpenoids comprise the largest class of natural products, with nearly 50 000 known members.[1] Underlying the astounding structural variation within this class of compounds are the diverse carbon backbone structures formed by terpene synthases/cyclases. These enzymes mediate complex electrophilic cyclizations and/or rearrangements that create these diverse skeletal structures from relatively simple acyclic isoprenoid precursors.[2] However, while the cyclization of triterpenes and many diterpenes are mechanistically similar in that they are initiated by protonation of a C=C double bond, identification and analysis of the genes for the relevant enzymes has revealed that there is no corresponding phylogenetic relationship. In particular, rather than being related to triterpene cyclases, these diterpene cyclases were found to be homologous to "lower" terpene synthases (TPS), which typically initiate catalysis by ionization of the allylic diphosphate ester bond in acyclic isoprenoid substrates, such as the universal diterpenoid precursor (*E,E,E*)-geranylgeranyl diphosphate (GGPP, **1**). Accordingly, TPSs can be divided into two mechanistically distinct groups, the prevalent class I enzymes, which catalyze diphosphate ionization-initiated reactions, and atypical class II enzymes, which catalyze protonation-initiated cyclization reactions.[2,3]

Structural and mechanistic studies of the common class I TPS enzymes have demonstrated that these synthases contain a characteristic aspartate-rich DDXXD motif that binds divalent metal ions required for catalysis of diphosphate ionization.[2,3] The first class II TPS identified, *ent*-copalyl/labdadienyl diphosphate (*ent*-CPP, **2**) synthase (CPS) from *Arabidopsis thaliana* (AtCPS), was found to lack this DDXXD motif, and instead contained a separately placed DXDD motif.[4] Despite the lack of any other homology, it was suggested that the AtCPS DXDD motif is important for class II catalysis based on the occurrence of a similar motif in previously identified squalene–hopene (triterpene) cyclases (SHC).[5] Structural and mechanistic studies have demonstrated that the DXDD motif in SHC, and the corresponding VXDC motif in oxidosqualene (sterol) cyclases (OSC), initiate cyclization with the "middle" aspartate, which is presumed to act as the catalytic acid. The other conserved residues are thought to "activate" this aspartate for protonation of the terminal C=C double bond of squalene (SHC) or corresponding epoxide ring of oxidosqualene (SHC or OSC).[5]

Class II TPS also characteristically contain a DXDD motif,[2] and mutational analysis has demonstrated that the DXDD motif in the bifunctional (i.e., class I and II) TPS abietadiene synthase (AS) is required for class II activity,[6,7] which is consistent with the suggestion that the DXDD motif in class II TPS also plays a role in initiating cyclization by protonating the terminal C=C double bond of GGPP. However, these studies also reported two important differences between the class II activity of AS and SHC/OSC. First, the class II activity of AS requires divalent metal ions (preferably Mg^{2+}),[7] whereas SHC and OSC do not.[8] Second, aza analogues that mimic the initial carbocations formed by protonation are very effective inhibitors of the class II activity of AS, but not SHC/OSC. Specifically, 14,15-dihydro-15-azaGGPP (15-azaGGPP, **3**) exhibits approximately nanomolar affinity for the class II active site of AS,[6] but the equivalent 2,3-dihydro-2-azasqualene exhibits much weaker (approximately micromolar) affinity for SHC/OSC.[9] These mechanistic differences, coupled with the lack of homology outside of this short motif, leave the role of the class II TPS DXDD motif in question. In particular, the DXDD motif represents a potential divalent metal binding site and synergistic Mg^{2+}–GGPP substrate inhibition effects have been interpreted to suggest a role for these aspartates in Mg^{2+} binding, as well as alternative GGPP binding modes.[10] Despite the importance of these enzymes in catalyzing the committed step in the biosynthesis of the large family of labdane-related diterpenoid natural products (which contains more than 5000 known members),[11] no direct evidence for the exact role of the DXDD motif in class II TPS catalysis has yet been presented.

To address this fundamental question, we report here mechanistic studies utilizing the known epoxy analogue of **1**, (±)-14,15-oxidogeranylgeranyl diphosphate (oxidoGGPP, **4**)[12] wherein the C14,15 double bond normally protonated to initiate cyclization is replaced by an epoxide ring (Scheme 1), in combination with site-directed mutational analysis of a recombinant pseudomature version of AtCPS (rAtCPS).[10] It seems reasonable to presume that oxidoGGPP will be more susceptible to protonation than GGPP given the known greater reactivity of oxidosqualene relative to squalene.[5] The increased basicity and strain energy of the epoxide relative to the C=C double bond translates into a less stringent requirement for activation of the catalytic acid. Thus, SHC, with its DXDD motif, can cyclize (i.e., protonate) either oxidosqualene or squalene, while OSC, with the less acidic VXDC motif, can cyclize/protonate only oxidosqualene and not squalene.[5] Structural analysis of both SHC and OSC has indicated that the absolutely conserved "middle" aspartate acts as the catalytic acid,[13,14] a conclusion confirmed by various mechanistic and mutational studies.[5] Of particular interest, mutation of the "last" aspartate of the DXDD motif in SHC led to compromised enzymes that were able to readily cyclize oxidosqualene, which has a more easily protonated epoxide ring, but were severely impaired with squalene, which contains the less basic

[a] *S. Prisic, Prof. Dr. R. J. Peters*
Department of Biochemistry, Biophysics, and Molecular Biology
Iowa State University, Molecular Biology Building
Ames, IA 50011 (USA)
Fax: (+1) 515-294-0453
E-mail: rjpeters@iastate.edu

[b] *Dr. J. Xu, Prof. Dr. R. M. Coates*
Department of Chemistry, University of Illinois
600 South Mathews Avenue, Urbana, IL 61801 (USA)

[c] *Dr. J. Xu*
Current address: Neurogen Corp.
Branford, CT 06405 (USA)

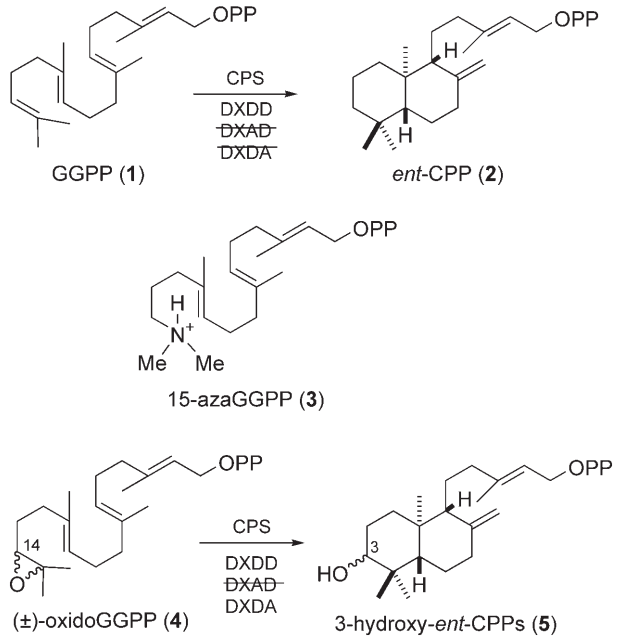

Scheme 1. Cyclization of GGPP (**1**) to *ent*-copalyl diphosphate (**2**), or (±)-oxidoGGPP (**4**) to a mixture of 3α- and 3β-hydroxy-*ent*-CPPs (**5**) by wild-type and/or mutant rAtCPS; strikeout indicates inactive mutant.

Table 1. Kinetic parameters of AtCPS and its mutants for GGPP. Observed rates were measured from reactions with 5 μM GGPP (**1**).

	V_{obs} [s^{-1}]	K_M [μM]	Reaction conditions
wild-type rAtCPS (DXDD)	1.2±0.1	2.9±0.8	12 nM enzyme, 30 s
rAtCPS:D379A (DX**A**D)	(7.1±0.5)×10^{-8}	16±11	4 μM enzyme, 41 h
rAtCPS:D380A (DXD**A**)	(4.1±1.7)×10^{-4}	5.4±1.6	1 μM enzyme, 30 min

C=C double bond.[15,16] This provided direct evidence that the "last" aspartate plays a critical role in activating the "middle" aspartate sufficiently to enable protonation of the terminal C=C double bond of squalene.

To begin investigating the role of the DXDD motif in class II TPS, we carried out kinetic analyses of wild-type rAtCPS to confirm the mechanistic differences relative to SHC/OSC activity reported with AS.[6,7] As previously reported, rAtCPS requires a divalent metal ion cofactor (preferably Mg^{2+}), and exhibits a ~1000-fold reduction in catalytic rate in the presence of EDTA.[10] In addition, rAtCPS is very effectively inhibited by 15-aza-GGPP (**3**), and exhibits near to nanomolar affinity (IC_{50} = 11 ± 3 nM). Further, substituting alanine for the "middle" and "last" aspartate of the DXDD motif resulted in mutant enzymes, rAtCPS:D379A and rAtCPS:D380A, respectively, that were effectively unable to cyclize GGPP (**1**) to *ent*-CPP (**2**). While the formation of **2** from **1** was detectable within 15 s with wild-type rAtCPS, even after 30 min incubations no product was formed from **1** with either the D379A or D380A mutants. With increased enzyme concentration and incubation time, it was possible to measure apparent catalytic rates for both mutants, which exhibited > 1000-fold reductions in apparent catalytic rate, with much less effect (less than sixfold) on the GGPP substrate pseudobinding constant, K_M (Table 1). This result reaffirms the importance of this motif for class II TPS enzymatic catalysis. These mutants were then used in conjunction with the oxidoGGPP (**4**) substrate analogue to probe the role of the corresponding aspartate residues.

It has previously been shown that the 14*R* and 14*S* enantiomers of (±)-**4** are converted to 3α- and 3β-hydroxy-*ent*-kaurene with cell-free extracts of wild cucumber (*Echinocystis macrocarpa*) that contain CPS and the subsequently acting kaurene synthase,[12] presumably via the corresponding stereoisomers of 3-hydroxy-*ent*-CPP (**5**). Incubation of **4** with wild-type rAtCPS yielded a major and minor product in a 3:2 ratio. The major product was identified to be 3α-hydroxy-*ent*-CPP by enzymatic dephosphorylation to 3α-hydroxy-*ent*-copalol and GC–MS comparison to an authentic sample of its enantiomer, (+)-3β-hydroxycopalol.[17] The almost identical mass spectrum of the minor product after dephosphorylation provided strong evi-

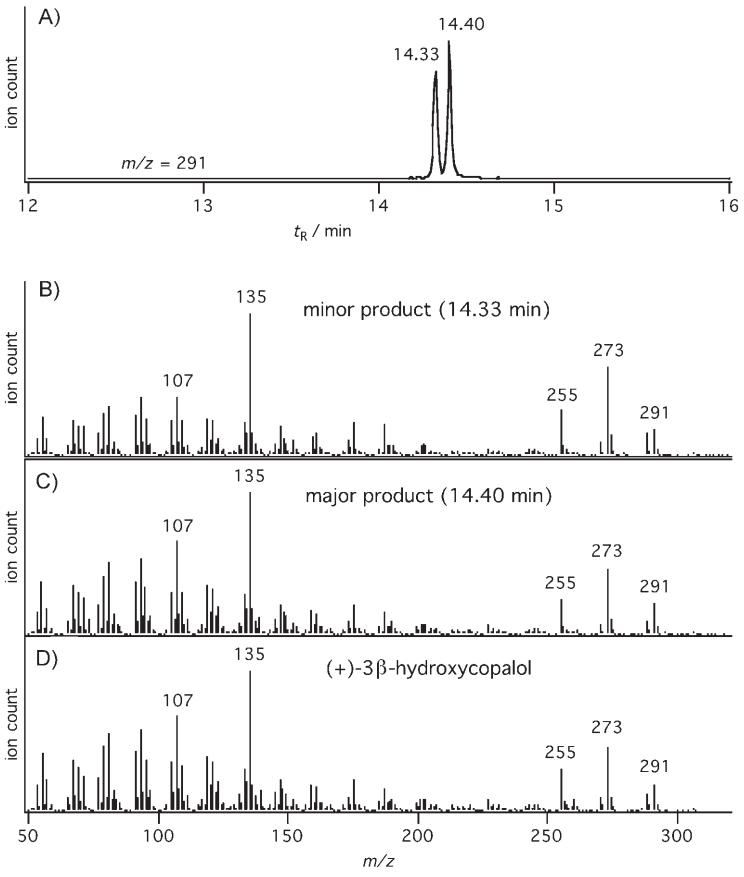

Figure 1. GC–MS analysis of dephosphorylated reaction products formed from oxidoGGPP by rAtCPS. A) Selected ion chromatogram (*m/z* 291); B) mass spectrum for the minor product (t_R = 14.33 min); C) mass spectrum for the major product (t_R = 14.40 min); D) mass spectrum for authentic (+)-3β-hydroxycopalol standard (t_R = 14.40 min).

dence for its assignment as the C3 epimer 3β-hydroxy-*ent*-CPP (Figure 1). In agreement with the previous results,[12] we also found that the rAtCPS products serve as substrates for recombinant kaurene synthase to yield 3α- and 3β-hydroxy-*ent*-kaurene. This result further supports the assigned structures (**5**) for the product obtained from the reaction between **4** and rAtCPS.

To probe the catalytic role of the class II TPS DXDD motif, we investigated the relative ability of the wild-type, D379A, and D380A variants of rAtCPS to react with oxidoGGPP (**4**). Notably, both wild-type and D380A rAtCPS readily cyclized **4**, whereas the D379A mutant remained essentially inactive—although it was possible to measure an apparent catalytic rate—and neither mutation had much effect (<threefold) on the oxidoGGPP (**4**) substrate pseudobinding constant, K_M (Table 2).

Table 2. Kinetic parameters of AtCPS and its mutants for oxidoGGPP. Observed rates were measured from reactions with 5 μM oxidoGGPP (**4**).

	V_{obs} [s^{-1}] for major product (3α-**5**)	K_M [μM]	Reaction conditions
wild-type rAtCPS (DXDD)	0.67 ± 0.09	1.7 ± 0.6	12 nM enzyme, 15 s
rAtCPS:D379A (DX**A**D)	$(7.7 \pm 0.3) \times 10^{-7}$	3.5 ± 2.8	4 μM enzyme, 41 h
rAtCPS:D380A (DXD**A**)	0.017 ± 0.003	1.5 ± 0.2	40 nM enzyme, 5 min

Thus, the D379A mutant was greatly impaired with both substrates, and exhibited ≥1 000 000-fold reductions in catalytic rate, while the D380A mutant exhibited differential effects on catalytic turnover of **1** (~40-fold reduction) and **4** (~3000-fold reduction), relative to wild-type rAtCPS.

3β-Hydroxy-*ent*-CPP remained the minor product in reactions with the D380A mutant (i.e., was not detected after 30 min incubation). However, 3β-hydroxy-*ent*-CPP was the major product of the D379A mutant ($V_{obs} = (2.9 \pm 0.1) \times 10^{-6}\ s^{-1}$). This indicates that, in the absence of a "middle" aspartate, the 14*S* substrate can be protonated by a different group. Results of experiments conducted with SHC, in which mutants of either the "first" or "middle" aspartate of the SHC DXDD motif could still cyclize oxidosqualene, and the double mutation of both completely abolished activity, suggest that either the "first" or "middle" aspartate can protonate this substrate.[16] We therefore speculate that the "first" aspartate in the DXDD motif of AtCPS protonates oxidoGGPP in the absence of the "middle" aspartate. However, we also note that mutation of the "middle" aspartate in rAtCPS had a more significant effect on catalytic rate than was observed with SHC.[16]

The results reported here for the class II TPS DXDD motif are qualitatively equivalent to those reported for mutational analyses of the SHC DXDD motif,[16] and strongly indicate that this aspartate-rich motif serves the same function. Specifically, the "last" aspartate is required to activate the "middle" aspartate sufficiently to protonate a terminal C=C double bond—albeit that of GGPP rather than squalene. Thus, the apparently unrelated class II TPS and SHC seem to utilize equivalent catalytic groups (i.e., the aspartate-rich DXDD motifs) to effect protonation of a terminal C=C double bond. This suggests the possibility of distant (i.e., structural) homology between the mechanistically similar triterpene and class II diterpene cyclases. Resolution of any such relationship awaits further studies that clarify the mechanism, in particular the observed differences relative to SHC/OSC, and especially structural information for class II TPS. The oxidoGGPP (**4**) substrate analogue utilized here will provide a valuable tool for future mechanistic studies that probe the role of other putative catalytic residues in the structurally undefined class II TPS. In addition, the results reported here are also potentially relevant to the proposed role of oxidoGGPP enantiomers in the biosynthesis of cyclic diterpenes oxygenated at the C3.[12,18]

Experimental Section

Preparation of (±)-14,15-oxido-GGPP (4)

General procedures: Solvents were distilled from the indicated drying agents prior to use: THF, diethyl ether, and benzene (Na/benzophenone); CH_2Cl_2 (CaH_2); hexane and ethyl acetate (none). CH_3CN and DMF were distilled from P_2O_5 and stored over 3 Å molecular sieves. Et_3N and pyridine were distilled from CaH_2 and stored over KOH. s-Collidine and methanesulfonyl chloride were obtained from Aldrich Chemical Co. and used without further purification. Dihydrogen disodium pyrophosphate was obtained from Sigma Chemical Co. and converted to $HOPP(NBu_4)_3$ according to a procedure reported by Woodside, Huang, and Poulter.[19]

The progress of reactions was followed by TLC unless stated otherwise. TLC analyses were performed on plastic-backed Merck Kieselgel 60 F254 plates, visualized by using UV fluorescence at 254 nm, I_2 stain, or phosphomolybdic acid stain (PMA, 10% in absolute ethanol), and developed on a hot plate at 120 °C. Dowex AG 50W-X8 ion-exchange resin (H^+ form) was obtained from BioRad and converted to the ammonium form before each chromatography experiment according to a published procedure.[19] Flash chromatography was performed according to the procedure of Mitra, Kahn, and Still[20] by using Merck 0.040–0.063 mm silica gel.

^1H NMR spectra were acquired either on a Unity 400 or 500 spectrometers at 400 or 500 MHz in $CDCl_3$ with $CHCl_3$ as the internal reference ($CHCl_3 = 7.26$ ppm), C_6D_6 with C_6D_5H as the internal reference ($C_6D_5H = 7.16$ ppm), or CD_3OD with CD_3OH as the internal reference ($CD_3OH = 4.78$ ppm). ^{31}P NMR spectra were recorded by using the Unity 400 at 162 MHz in CD_3OD with H_3PO_4 (85%) as the external reference ($H_3PO_4 = 0.00$ ppm).

(E,E,E)-Geranylgeranyl acetate: Acetylation was carried out according to published procedures.[21,22] Treatment of (*E,E,E*)-geranylgeraniol (0.250 g, 0.862 mmol)[23,24] with acetic anhydride (0.528 g, 5.172 mmol) in dry pyridine (3 mL) was conducted at room temperature under N_2 for 21 h. The product was isolated by ether extraction and obtained as a colorless oil; yield 0.277 g (97%).

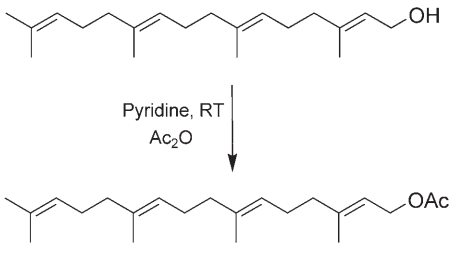

(±)-(E,E,E)-14-Bromo-15-hydroxy-14,15-dihydrogeranylgeranyl acetate: The terminal hypobromination reaction was carried out according to published procedures.[21,22] (*E,E,E*)-Geranylgeranyl acetate (0.277 g, 0.834 mmol) was treated with *N*-bromosuccinimide (0.163 g, 0.918 mmol) in THF/H_2O (7.4 mL/5.0 mL) at 0 °C for 3 h, the cloudy solution was diluted with water (30 mL), and the product was extracted with ether (30 mL × 3). Purification by flash chromatography on a silica gel column (25:75 ethyl acetate/hexanes as eluent) gave the bromohydrin as a clear oil; yield 0.208 g (58%); TLC $R_f = 0.43$ (ethyl acetate/hexanes 25:75). The ^{1}H and ^{13}C NMR data agreed with the literature values.[21,25]

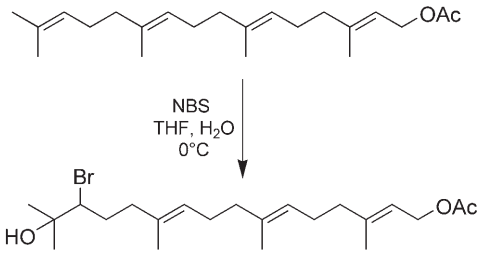

(±)-(E,E,E)-14,15-Oxidogeranylgeraniol: This reaction was carried according to published procedures.[21,22] A solution of bromohydrin (0.208 g, 0.485 mmol) in MeOH (12 mL) was stirred at room temperature as solid K_2CO_3 (0.516 g, 3.73 mmol) was added. After 2 h, water (25 mL) was added, the product was extracted with hexanes (50 mL × 4), and the combined organic phases were dried with anhydrous $MgSO_4$. The solvent was removed by rotary evaporation. Purification by flash chromatography on a silica-gel column (25:75 ethyl acetate/hexanes as eluent) gave the epoxy alcohol as a colorless liquid; yield 0.126 g (85%); TLC $R_f = 0.20$ (ethyl acetate/hexanes 25:75); IR (CH_2Cl_2) 3400 cm^{-1} (OH); ^{1}H NMR (400 MHz, CD_3OD): $\delta =$ 5.22 (t, $J = 6.4$ Hz, 1H; =CH), 5.03 (t, $J = 7.0$ Hz, 1H; =CH), 5.00 (t, $J = 7.5$ Hz, 1H; =CH), 3.94 (d, $J = 6.8$ Hz, 2H; CH_2OH), 2.60 (t, $J = 6.3$, 1H), 1.97 (m, 4H), 1.87 (m, 6H), 1.52 (s, 3H), 1.48 (s, 3H), 1.47 (s, 3H), 1.44–1.50 (m, 2H), 1.13 (s, 3H), 1.11 (s, 3H); ^{13}C NMR (100 MHz, CD_3OD): $\delta = 138.0$, 135.4, 134.7, 125.6, 125.5, 125.0, 64.1, 59.6, 58.1, 40.4, 40.3, 37.2, 28.3, 27.3, 27.1, 25.3, 19.2, 16.6, 16.4 ppm. The ^{1}H and ^{13}C NMR data agreed with the literature values.[21,25]

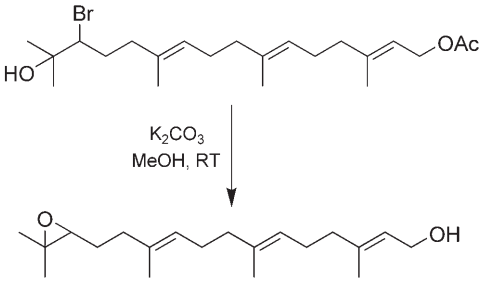

(±)-(E,E,E)-14,15-Oxidogeranylgeranyl chloride: Conversion to the chloride was carried out according to the procedure of Corey and Shieh[26] with slight modification. The epoxy alcohol (0.020 g, 0.065 mmol) was placed in a dry vial (10 mL) with a stirring bar. The vial was sealed with a septum and purged with N_2, and CH_2Cl_2 (0.16 mL) was added by using a syringe. The solution was stirred and cooled to −45–−40 °C in a CH_3CN/dry ice bath, and Et_3N (0.0092 g, 0.091 mmol) and CH_3SO_2Cl (0.0089 g, 0.078 mmol) were added sequentially by using a syringe. After 30 min, a suspension of LiCl (0.069 g, 0.1625 mmol) partially dissolved in THF (0.20 mL) was added by using a pipette, the septum was replaced, and the CH_3CN/dry ice bath was changed to an ice-water bath. The suspension was stirred at 0 °C for 1 h, poured into ice-water (20 mL), and extracted with hexane (50 mL × 4). The organic extracts were combined and washed with saturated $NaHCO_3$ (10 mL × 3) and brine (10 mL × 2), and dried over $MgSO_4$. Removal of the solvent by rotary evaporation gave the epoxy chloride as a colorless oil; yield 20 mg (94%); ^{1}H NMR (400 MHz, C_6D_6): $\delta = 5.35$ (t, $J = 7.9$ Hz, 1H; = CH), 5.24 (t, $J = 6.1$ Hz, 1H; =CH), 5.14 (t, $J = 7.1$ Hz, 1H; =CH), 3.79 (d, $J = 8.0$ Hz, 2H; CH_2Cl), 2.57 (t, $J = 6.3$ Hz, 1H; CHOC), 2.00–2.18 (m, 10H), 1.90 (t, $J = 7.5$ Hz, 2H), 1.56 (s, 3H), 1.55 (s, 3H), 1.54 (s, 3H), 1.15 (s, 3H), 1.10 ppm (s, 3H).

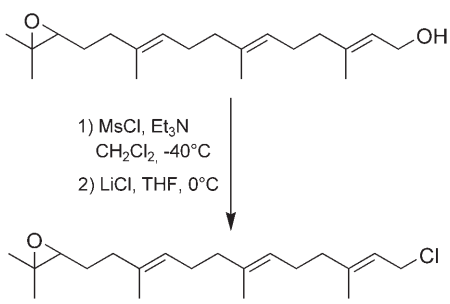

*(±)-(E,E,E)-14,15-Oxidogeranylgeranyl diphosphate (**4**)*: Diphosphate formation was carried out according to the method of Woodside, Huang, and Poulter.[19] Ion-exchange chromatography and purification procedures were carried out according to methods developed at the UIUC.[27] Epoxy chloride (0.050 g, 0.152 mmol) and dry molecular sieves (3 Å, 0.75 g) were placed in a dry vial equipped with a stirring bar. Dry CH_3CN (2.0 mL) and $HOPP(NBu_4)_3$ (0.280 g, 0.304 mmol) were then added quickly. The vial was sealed with a septum and purged with N_2. The suspension was stirred at room temperature for 15 h. The solids were removed by filtration and washed with CH_3CN (70 mL). The CH_3CN filtrate was washed with pentane (10 mL × 3), and CH_3CN was removed with a rotary evaporator. The remaining trisammonium salt was dissolved in elution solution (18 mL) and passed through an ion-exchange column (diameter: 1.2 cm, height: 25 cm, volume: 30 mL) with elution solution (52 mL; see below). The resin (30 mL BIO-RAD® AG 50W-X8) was freshly washed before use with saturated NH_4OH and deionized water until it was at pH 7.0. The elution solution was NH_4HCO_3 (0.2%, *w/v*) and isopropyl alcohol (2%, *v/v*) in H_2O. The total eluate was collected in a round-bottomed flask and frozen as it was rotated in a dry ice/isopropyl alcohol bath, and lyophilized for 3 h. The lyophilization was then stopped, and the flask was vented slowly and carefully, and water (5 mL) was added to dissolve all the solids. The resulting partially frozen solution was allowed to thaw at room temperature, frozen while being rotated in a dry ice/isopropyl alcohol bath, and lyophilized again. The lyophilization was repeated twice to afford a minimum amount of crude white powder. The crude white powder was transferred to a centrifuge tube with dry MeOH (8 mL), vortexed, and centrifuged. The supernatant was transferred and concentrated to 0.5–0.6 mL by rotary evaporation. Dry MeOH (8 mL) was again added to the remaining solids in the centrifuge tube, and the resulting suspension was vortexed and centrifuged. The supernatant was concentrated to 0.5–0.6 mL by rotary evaporation. This extraction/vortex/centrifugation/concentration procedure was repeated twice. ^{31}P NMR analysis of the four supernatant fractions was conducted to determine the ratio of prod-

uct diphosphate (2d, δ_P = ca. −8, −9 ppm) to inorganic pyrophosphate (s, δ_P = +3 ppm). Combination and lyophilization of supernatant fractions 1 and 2 afforded the epoxy diphosphate as a white powder; yield 22 mg (48%, 72% purity, the major impurity was $HOPO_3^{2-}$); ^{31}P NMR (376 MHz, CD_3OD): δ = −8.25 (d, J = 19.5 Hz, 1P), −8.78 ppm (d, J = 19.8 Hz, 1P); ^1H NMR (400 MHz, CD_3OD): δ = 5.32 (t, J = 5.7 Hz, 1H; =CH), 5.06 (t, J = 6.4 Hz, 1H; =CH), 5.02 (t, J = 6.6 Hz, 1H; =CH), 4.41 (t, J = 6.0 Hz, 2H; CH_2OPP), 2.64 (t, J = 6.2 Hz, 1H; CHOC), 1.87–2.01 (m, 12H), 1.58 (s, 3H), 1.52 (s, 3H), 1.50 (s, 3H), 1.17 (s, 3H), 1.14 ppm (s, 3H).

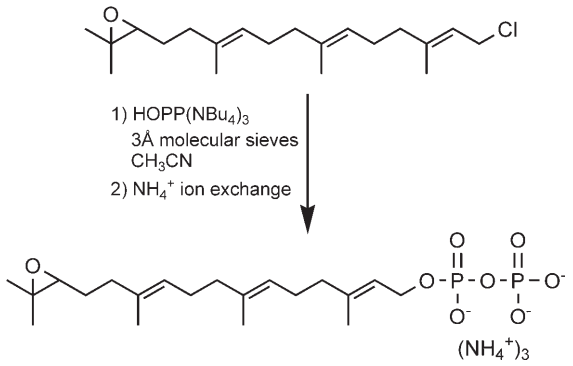

rAtCPS expression, purification, and characterization

General procedures: Unless otherwise noted all chemicals were purchased from Fisher Scientific (Loughborough, Leicestershire, UK) and molecular biology reagents were obtained from Invitrogen (Carlsbad, CA).

Gas chromatography (GC) was performed with an Agilent 6890N GC instrument (Palo Alto, CA) by using an HP-1 column with flame ionization detection (FID), or an HP-5 column with mass spectrometry (MS) detection on a GC equipped with a 5973N mass selective detector in electron-ionization mode (70 eV; W. M. Keck Metabolomics Research laboratory, Iowa State University). Samples (5 μL) were injected at 40 °C in splitless mode, the oven temperature was maintained at 40 °C for 3 min, then increased to 300 °C at a rate of 20 °C min^{-1}, and maintained for 3 min. MS data were collected from 50 to 500 *m/z* during the temperature ramp and final hold.

Expression and purification: Recombinant pseudomature rAtCPS was obtained by expression of AtCPS, which lacks the first 84 amino acids, by using the Gateway system pDEST14 expression vector in the OverExpress™ C41(DE3) strain of *E. coli* (Lucigen; Middleton, WI, USA) as previously described.[10] Briefly, expression was carried out and soluble extract was obtained as described,[28] and rAtCPS was initially purified over ceramic hydroxyapetite and HQ columns by using a BioLogic LP chromatography system (BioRad). The resulting preparation was desalted on a small hydroxyapetite column prior to purification over a MonoQ column by using an AKTAfplc system (Amersham). The resulting ~98% pure rAtCPS was dialyzed against BisTris (10 mM, pH 6.8), DTT (2 mM), glycerol (10%), and stored at 4 °C for up to 10 days, or at −80 °C for several months without significant loss in activity.

Site directed mutagenesis: Site-directed mutagenesis to construct rAtCPS:D379A and rAtCPS:D380A was carried out by using PCR amplification of the Gateway system pENTR–rAtCPS cloning vector with overlapping mutagenic primers. The resulting mutant genes were verified by complete sequencing, and then transferred to pDEST14 by directional recombination for expression and purification as described above.

Enzymatic assays: All assays were performed as described.[10] Briefly, reactions (1 mL) were carried out at 30 °C in assay buffer (50 mM HEPES, pH 7.75, 100 mM KCl, 10% glycerol, 0.1 mM Mg^{2+}). Reactions were terminated by adding *N*-ethylmaleimide (20 mM) in glycine (500 mM, pH 11; 110 μL) and incubated at 75 °C for 5 min. Excess *N*-ethylmaleimide was deactivated by the addition of DTT (1 M; 20 μL) and samples were incubated for 15 min at room temperature. The samples were then neutralized with HCl (1 M; 60 μL). $ZnCl_2$ and $MgCl_2$ (final concentrations 10 mM and 100 mM, respectively; 12 μL) were added before the addition of bovine alkaline phosphatase (2 units; Promega) to dephosphorylate both substrates and products. The samples were then either incubated at room temperature, overnight, or at 37 °C for 2 h. The resulting aqueous solutions were extracted with hexanes (1 mL × 3), and the extracts were pooled, dried under N_2, and resuspended in hexanes (25 μL) for GC analysis. The stereospecific production of *ent*-CPP from GGPP (**1**) was verified by using GC–MS comparison with an authentic standard of *ent*-copalol, as previously described.[29,30] The major product from oxidoGGPP (**4**) was also identified by using GC–MS based comparison. In coupled assays with kaurene synthase, the original pair of peaks disappeared and a new pair, the mass spectra of which matched those of authentic epimeric forms of 3-hydroxy-*ent*-kaurene,[12,31] were observed. After initial product verification, GC–FID was used to quantify catalytic turnover. For these kinetic analyses enzyme concentrations and time of incubation were varied to achieve 2–8% turnover for GGPP (**1**) and 10–15% of the major product (3α-hydroxy-*ent*-CPP) for oxidoGGPP (**4**). To correct for handling errors, we determined catalytic rates from the observed fractional turnover (i.e., the ratio of product to the sum of product and substrate), along with the known starting concentration of GGPP (Sigma–Aldrich). Kinetic parameters were calculated by fitting the observed data to the substrate inhibition equation (KaleidaGraph 4.0; Synergy Software, Reading, PA, USA). For all curves the fit R^2 was 0.93–0.99.

Even though oxidoGGPP is presumably easier to protonate, and observed rates for its cyclization might be expected to be higher than those for GGPP (**1**), we observed that the epoxide analogue (**4**) was significantly less stable than **1** and appeared to be nonenzymatically converted to side products, which led to slower observed catalytic rates. For example, even in buffer (i.e., in the absence of enzyme) 1–2% of oxidoGGPP was converted to a product with a distinct mass spectrum but very similar retention time to 3β-hydroxy-*ent*-copalol, and ~6% was converted to a byproduct with slightly lower retention time than 3α-hydroxy-*ent*-copalol in 30 min. Note that the catalytic rates reported here were calculated after correction for these nonenzymatic reactions. The mass spectra for both dephosphorylated byproducts were similar and resembled that generated after dephosphorylation of oxidoGGPP (**4**); this finding suggests the presence of acyclic structures. One byproduct might be the ketone arising from 14,15 hydride shift, that is, 14-oxo-14,15-dihydroGGPP, as ketone byproducts that result from hydride shift often accompany Lewis-acid-initiated cyclizations of epoxypolyenes.[22] Alternatively, the byproduct might arise from hydrolysis of the epoxide ring, that is, 14,15-dihydroxy-14,15-dihydroGGPP. By contrast, GGPP was significantly more stable, with no detectable formation of CPP even after incubations for up to 3 days (72 h) in the absence of enzyme; this procedure enabled the measurement of the very slow catalytic rates reported here (e.g., for the rAtCPS:D379A mutant).

Acknowledgements

This work was supported by grants from the National Science Foundation (MCB-0416948 to R.J.P.) and National Institutes of Health (GM076324 to R.J.P. and GM13956 to R.M.C.).

Keywords: diterpene cyclases · DXDD motif · enzyme catalysis · isomerases · protonation

[1] J. Buckingham, *Dictionary of Natural Products*, on-line edition, Chapman & Hall/CRC, **2002**.
[2] D. W. Christianson, *Chem. Rev.* **2006**, *106*, 3412 – 3442.
[3] K. U. Wendt, G. E. Schulz, *Structure* **1998**, *6*, 127 – 133.
[4] T.-P. Sun, Y. Kamiya, *Plant Cell* **1994**, *6*, 1509 – 1518.
[5] K. U. Wendt, G. E. Schulz, E. J. Corey, D. R. Liu, *Angew. Chem.* **2000**, *112*, 2930 – 2952; *Angew. Chem. Int. Ed.* **2000**, *39*, 2812 – 2833.
[6] R. J. Peters, M. M. Ravn, R. M. Coates, R. B. Croteau, *J. Am. Chem. Soc.* **2001**, *123*, 8974 – 8978.
[7] R. J. Peters, R. B. Croteau, *Biochemistry* **2002**, *41*, 1836 – 1842.
[8] E. J. Corey, H. Cheng, C. H. Baker, S. P. T. Matsuda, D. Li, X. Song, *J. Am. Chem. Soc.* **1997**, *119*, 1277 – 1288.
[9] F. Viola, M. Ceruti, L. Cattel, P. Milla, K. Poralla, G. Balliano, *Lipids* **2000**, *35*, 297 – 303.
[10] S. Prisic, R. J. Peters, *Plant Physiol.* **2007**, DOI: 10.1104/pp.106.095208
[11] M. Xu, M. L. Hillwig, S. Prisic, R. M. Coates, R. J. Peter, *Plant J.* **2004**, *39*, 309 – 318.
[12] R. M. Coates, R. A. Conradi, D. A. Ley, A. Akeson, J. Harada, S. C. Lee, C. A. West, *J. Am. Chem. Soc.* **1976**, *98*, 4659 – 4660.
[13] K. U. Wendt, K. Poralla, G. E. Schulz, *Science* **1997**, *277*, 1811 – 1815.
[14] R. Thoma, T. Schulz-Gasch, B. D'Arcy, J. Benz, J. Aebi, H. Dehmlow, M. Henning, M. Stihle, A. Ruf, *Nature* **2004**, *432*, 118 – 122.
[15] T. Dang, G. D. Prestwich, *Chem. Biol.* **2000**, *7*, 643 – 649.
[16] T. Sato, T. Hoshino, *Biosci. Biotechnol. Biochem.* **1999**, *63*, 2189 – 2198.
[17] N. K. N. Yee, R. M. Coates, *J. Org. Chem.* **1992**, *57*, 4598 – 4608.
[18] C. Durr, H.-J. Schnell, A. Luzhetskyy, R. Murillo, M. Weber, K. Welzel, A. Vente, A. Bechthold, *Chem. Biol.* **2006**, *13*, 365 – 377.
[19] A. B. Woodside, Z. Huang, C. D. Poulter, *Org. Synth. Coll.* **1993**, *VIII*, 616 – 620.
[20] A. Mitra, M. Kahn, W. C. Still, *J. Org. Chem.* **1978**, *43*, 2923 – 2925.
[21] M. M. Ravn, PhD dissertation, University of Illinois (USA), **2000**.
[22] E. E. VanTamelen, R. G. Nadeau, *Bioorg. Chem.* **1982**, *11*, 197 – 218.
[23] R. W. Sum, L. Weiler, *Tetrahedron* **1981**, *37*, 303 – 317.
[24] Y. Jin, F. G. Roberts, R. M. Coates, *Org. Synth.* **2007**, *84*, 43 – 57.
[25] S.-I. Takanashi, K. Mori, *Liebigs Ann./Recl.* **1997**, 828 – 838.
[26] E. J. Corey, W.-C. Shieh, *Tetrahedron Lett.* **1992**, *33*, 6435 – 6438.
[27] Y. Zhao, PhD dissertation, University of Illinois (USA), **2005**.
[28] R. J. Peters, J. E. Flory, R. Jetter, M. M. Ravn, H.-J. Lee, R. M. Coates, R. B. Croteau, *Biochemistry* **2000**, *39*, 15 592 – 15 602.
[29] S. Prisic, M. Xu, P. R. Wilderman, R. J. Peters, *Plant Physiol.* **2004**, *136*, 4228 – 4236.
[30] L. J. Harris, A. Saparno, A. Johnston, S. Prisic, M. Xu, S. Allard, A. Kathiresan, T. Ouellet, R. J. Peters, *Plant Mol. Biol.* **2005**, *59*, 881 – 894.
[31] D. Ley, PhD dissertation, University of Illinois (USA), **1976**.

Received: January 29, 2007
Published online on April 24, 2007

